**Annales
Geophysicae**

The ionospheric responses to the 11 August 1999 solar eclipse: observations and modeling

H. Le[1,2], L. Liu[1], X. Yue[1,2], and W. Wan[1]

[1]Institute of Geology and Geophysics, Chinese Academy of Sciences, Beijing 100029, China
[2]Graduate School of the Chinese Academy of Sciences, Beijing 100049, China

Abstract. A total eclipse occurred on 11 August 1999 with its path of totality passing over central Europe in the latitude range 40°–50° N. The ionospheric responses to this eclipse were measured by a wide ionosonde network. On the basis of the measurements of foE, foF1, and foF2 at sixteen ionosonde stations in Europe, we statistically analyze the variations of these parameters with a function of eclipse magnitude. To model the eclipse effects more accurately, a revised eclipse factor, F_R, is constructed to describe the variations of solar radiation during the solar eclipse. Then we simulate the effect of this eclipse on the ionosphere with a mid- and low-latitude ionosphere theoretical model by using the revised eclipse factor during this eclipse. Simulations are highly consistent with the observations for the response in the E-region and F1-region. Both of them show that the maximum response of the mid-latitude ionosphere to the eclipse is found in the F1-region. Except the obvious ionospheric response at low altitudes below 500 km, calculations show that there is also a small response at high altitudes up to about 2000 km. In addition, calculations show that when the eclipse takes place in the Northern Hemisphere, a small ionospheric disturbance also appeared in the conjugate hemisphere.

Keywords. Ionosphere (Mid-latitude ionosphere; Modeling and forecasting)

1 Introduction

Solar eclipses provide unique opportunities to study the behavior of the ionosphere. During a solar eclipse, the Moon's shadow decreases the ionizing radiation from the Sun, causing changes in electron concentration and temperature, and neutral compositions and temperature. During the past decades, the responses of the ionosphere to solar eclipses have been studied extensively with various methods, such as the Faraday rotation measurement, ionosonde network, incoherent scatter radar (ISR), Global Positioning System (GPS), and satellite measurements (e.g. Evans, 1965a, b; Klobuchar and Whitney, 1965; Rishbeth, 1968; Hunter et al., 1974; Oliver and Bowhill, 1974; Cohen, 1984; Salah et al., 1986; Cheng et al., 1992; Tsai and Liu, 1999; Huang et al., 1999; Afraimovich et al., 1998, 2002; Farges et al., 2001, 2003; Tomás et al., 2007; Adeniyi et al., 2007). These studies have shown that there is almost a consistent behavior in the low altitudes where electron density drops by a large percentage during a solar eclipse, whereas the F2-region behavior may be quite complicated during different eclipse events, showing either an increase or decrease in electron density. In addition, responses of the low-latitude and equatorial ionosphere may be quite different from those in the middle ionosphere. Huang et al. (1999) used a low-latitude ionospheric tomography network (LITN) to observe the ionospheric response to the solar eclipse of 24 October 1995 and found an enhancement, a depression, followed by an enhancement and depression in Total Electron Content (TEC). During the same eclipse event, there might be different ionospheric responses in different locations because of the differences in background parameters.

The total eclipse of 11 August 1999 occurred with its path of totality passing over central Europe at the latitude range 40°–50° N. The ionospheric responses to this eclipse were measured by a wide ionosonde network. There have been many studies on this eclipse in the past (e.g. Davis et al., 2000; Altadill et al., 2001; Afraimovich et al., 2002; Farges et al., 2003; Baran et al., 2003). In this paper, taking advantage of the dense network of geophysical observatories in Europe, we perform a statistical analysis to study the difference between the behaviors of the E- and F1-region during this eclipse for the first time. We also modelled the spatial and temporal patterns of the mid-latitude ionospheric response

Correspondence to: L. Liu
(liul@mail.iggcas.ac.cn)

Table 1. Locations of the ionosonde stations used during the eclipse measurements and their maximum solar obscuration at 200 km height.

Station	Geographic Latitude	Geographic Longitude	Maximum obscuration at 200 km height (%)
Salekhard	66.5° N	66.7° E	18.8
Novosibirsk	54.6° N	83.2° E	21.6
Lycksele	64.62° N	18.76° E	45.8
Leningrad	59.95° N	30.7° E	50.5
El Arenosillo	37.1° N	6.7° E	54.1
Moscow	55.5° N	37.3° E	56.4
Uppsala	59.8° N	17.6° E	58.8
Tortosa	40.4° N	0.3° E	68.5
Ashkhabad	37.9° N	58.3° E	74.7
Rostov	47.2° N	39.7° E	75.9
Juliusruh	54.6° N	13.4° E	77.2
Rome	41.8° N	12.52° E	81.1
San Vito	40.7° N	17.9° E	82.2
Fairford	51.7° N	1.8° E	93.6
Chilton	51.6° N	1.3° W	93.6
Sofia	42.7° N	23.4° E	94.9

to the total solar eclipse in terms of a mid- and low-latitude ionosphere theoretical model. In the past, there have been some studies on the ionospheric response to solar eclipses on the basis of numerical simulations (e.g. Stubbe, 1970; Roble et al., 1986; Müller-Wodarg et al., 1998; Boitman et al., 1999; Liu et al., 1999; Korenkov et al., 2003a, 2003b). However, they only considered the occultation of the photosphere being shielded by the Moon for variations in solar radiation during a solar eclipse. According to their method, the solar radiation should be zero when the photosphere is totally obscured, which would introduce some errors, especially in the low altitudes, because even at totality there are still some radiations from the unmasked part of solar corona (Rishbeth, 1968; Davis et al., 2000; Curto et al., 2006). In this paper, according to the astronomical model of Curto et al. (2006), we construct a revised eclipse factor to describe the variation of solar radiation during a solar eclipse. Unlike earlier studies mentioned above, in addition to the response of the ionosphere in the Northern Hemisphere during the eclipse, we also find the ionospheric disturbance in the conjugate hemisphere.

2 Data source

The total eclipse of 11 August 1999 occurred with its path of totality passing over central Europe in the geographic latitude range 40° N–50° N. The eclipse occurred during a relatively long geomagnetic quiet period. The eclipse therefore provides a unique opportunity to study the mid-latitude ionospheric response to the variation of solar EUV radiation. The

ionospheric responses to this eclipse were monitored by a wide ionosonde network. To examine the variations of the eclipse effects with the eclipse magnitude, which is defined as the fraction of the Sun's diameter occulted by the Moon, we performed a statistical analysis of the critical frequency of the ionospheric E and F1 layer, foE and foF1, from 16 ionosonde stations. These stations are listed in Table 1, in the order of maximum obscuration. The maximum obscuration at 200 km altitude over each station ranges from around 20% to 95% as shown in Table 1. A mean of thirty days is used as a reference on the control day for comparing the ionospheric behavior of the E and F1 layer during the eclipse with the normal behavior. The ionosonde data often only have a time resolution of one hour or half an hour. So we calculate the obscuration at the time near totality when foE or foF1 is available. Following a similar approach as Davis et al. (2000) and Curto et al. (2006), we calculated the relative changes in the peak electron density of the E layer and F1 layer, NmE_E/NmE_C and $NmF1_E/NmF1_C$, as a function of the fraction of the Sun's photosphere area unmasked by the Moon, SP_E/SP_C as seen at the height of 200 km, where NmE_E and $NmF1_E$ are the peak electron densities of the E layer and F1 layer on the eclipse day, NmE_C and $NmF1_C$ are the peak electron densities of the E layer and F1 layer on the control day, SP_E is the Sun's photosphere area unmasked by the Moon during the eclipse, SP_C is the Sun's photosphere area before and after the eclipse. The values of SP_E/SP_C can be obtained by astronomical calculation. According to the algorithm of Curto et al. (2006), the unmasked fraction of the total solar ionizing radiation drops to a minimum of about 22% of the value before eclipse at totality ($SP_E/SP_C=0$),i.e. the relative unmasked flux fraction of solar ionizing radiation is always larger than the unmasked area fraction of the Sun's corona over the photosphere (SP_E/SP_C), because some of the radiations come from the Sun's coronal layer. It should be noted that at a given ionosonde station, not all three parameters (foE, foF1, and foF2) were recorded during the eclipse of 11 August 1999. Among the 16 ionosonde stations, there are 12 records of foE and 13 records of foF1.

3 Ionospheric model and solar radiation during an eclipse

On the basis of previous works (Tu et al., 1997; Liu et al., 1999; Lei et al., 2004a, b), we develop a middle- and low-latitude theoretical ionospheric model, known as: the Theoretical Ionospheric Model of the Earth in the Institute of Geology and Geophysics, Chinese Academy of Sciences (TIME-IGGCAS) (Yue et al., 2008). This model uses an eccentric dipole approximation to the Earth's magnetic field. It solves the coupled equations of the mass continuity, momentum, and energy of three main ions O^+, H^+ and He^+ in closed geomagnetic tubes, with their footpoints anchored at about 100-km altitude to yield values of concentrations,

temperature, and field-aligned diffusion velocities of three main ions. The model also calculates the values of concentrations of three minor ions N_2^+, O_2^+ and NO^+ under the assumption of photochemical equilibrium.

The production rates of ions include the photoionization rates and chemical reaction production rates. The solar EUV radiation spectrum reported by Richards et al. (1994) is used to calculate the photoionization rates of the neutral gas O_2, N_2 and O. The secondary ionization effect of daytime photoelectron and several nighttime ionization sources are also considered. The loss rates of ions include chemical reaction loss and ion recombination loss. In the model 20 chemical reactions are considered. Detailed descriptions of chemical reactions and their reaction coefficient and collision frequencies can be found in the paper of Lei et al. (2004a).

The differences between the temperatures of different ions are assumed to be small; to obtain a faster calculation speed possible differences in the ion temperature are ignored in the model. We only calculate the O^+ temperature. The heating sources for electrons considered include photoelectron heating, elastic collision with neutral particles (N_2, O_2 and O), vibrational and rotational excitation of N_2 and O_2, excitation of the fine structure levels of atomic oxygen, excitation from 3P to 1-D state for atomic oxygen, and the energy transfer by electron-ion collisions; for the O^+, ion-electron collisions, ion-ion collisions and elastic and inelastic collisions with the neutrals are considered. For the lower boundary, the O^+ temperature equals the neutral temperature and the electron's temperature is obtained under the heat equilibrium assumption. The energy equations of the electron and O^+ are solved by the same finite difference method as that of the mass continuity equation (Lei, 2005). The reader is referred to the paper of Lei (2005) for detailed descriptions of the above-mentioned heating rates. The photoelectron heating effect is considered as that of Millward (1993).

The neutral temperature and densities are taken from the NRLMSIS-00 (Picone et al., 2002), and NO density is calculated from an empirical model developed by Titheridge (1997). The neutral winds are determined by the HWM-93 model (Hedin et al., 1996). In this study, we do not consider the possible effects of the solar eclipse on neutral atmospheric compositions and temperature, as well as neutral wind velocities.

During a solar eclipse, the solar radiation reaching the top of the Earth's atmosphere decreased in intensity because the Sun was obscured by the shadow of the Moon. To model the eclipse effects, the spectrum of solar radiation should be multiplied by an eclipse factor $F(UT, h, \Phi, \theta)$. UT is the universal time, h the altitude, Φ the geographic longitude, and θ the geographic latitude. There are some studies on the ionospheric response to solar eclipse on the basis of the numerical simulations in the past (e.g. Stubbe, 1970; Roble et al., 1986; Müller-Wodarg et al., 1998; Boitman et al., 1999; Liu et al., 1999; Korenkov et al., 2003a, b). However, for the variations of solar radiation during a solar eclipse, they
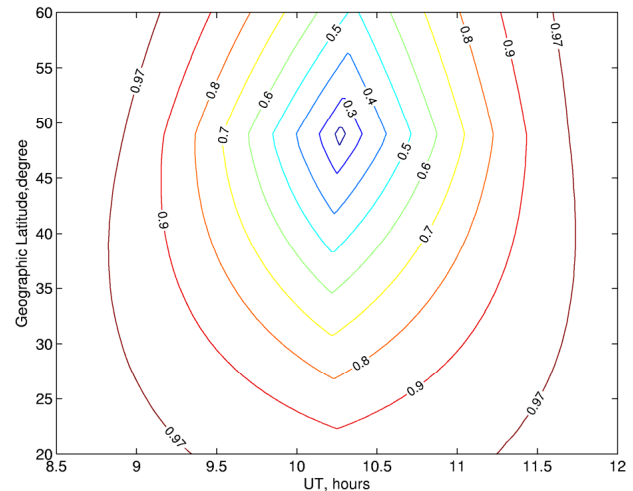

Fig. 1. Contours of the revised eclipse factor, $F_R(UT, h, \Phi, \theta)$, as a function of universal time (UT) and geographic latitude for an altitude of 200 km in the 1.67° E meridian during the solar eclipse of 11 August 1999.

only considered the occultation of the photosphere, i.e. in their simulations the value of $F(UT, h, \Phi, \theta)$ is defined as the unmasked fraction of the area of the Sun's photosphere. According to this method, the solar radiation would be zero at totality when the photosphere is totally obscured and one in the case of a non-eclipse. But it is well known that some of the solar soft-X-ray and EUV radiation which originate from the limb solar corona is not obscured during an eclipse (Rishbeth, 1968; Davis et al., 2000, 2001; Curto et al., 2006). Davis et al. (2000) presented a method, for the first time, for estimating the percentage of the ionising solar radiation which remains unobscured at any time during the eclipse by comparing the variation of the ionospheric E-layer with the behaviors of the layer during a control day and found that the flux of solar ionising radiation fell to a minimum of 25±2% of the value before and after the eclipse for the 11 August 1999 eclipse. The relative apparent sizes of the Moon and the Sun (photosphere) are different for each eclipse. Davis et al. (2001) discussed the effects on the unmasked solar radiation caused by the relative size of the Moon with respect to the solar disk, as the obscuration of chromospheric radiation is a sensitive function of this value: the larger the ratio of radii, the fewer the unmasked radiation. For the eclipse of 11 August 1999, the ratio of radii was 1.0277. Following a similar approach as Davis et al. (2000), Curto et al. (2006) evaluated the contribution of the radiation from different parts of the Sun in the Earth's ionosphere by using foE (critical frequency of E layer) data from many ionosonde stations and constructed an astronomical model to forecast the ionizing flux at any moment during the 11 August 1999 eclipse. The computation from the astronomical model shows that about 22% of the radiation was unmasked at eclipse totality for that
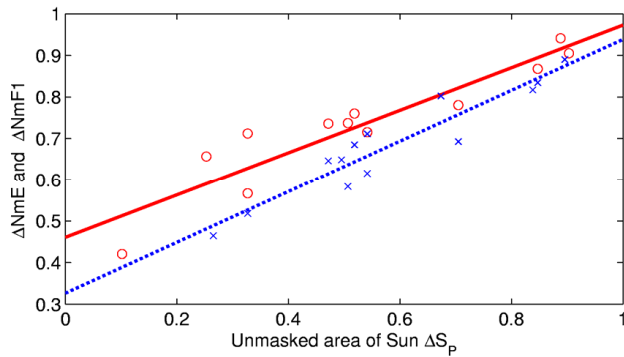
Fig. 2. Scatterplots of ΔNmE (circles) and ΔNmF1 (crosses) versus ΔS$_p$ and a linear fit for these observations (solid line for ΔNmE; dashed line for ΔNmF1).

eclipse event, which is in accord with the result of Davis et al. (2000). In this study, we define a revised eclipse factor F_R(UT, h, Φ, θ) as the ratio of the unmasked solar radiation to the total solar radiation including the radiation originating both in the photosphere and in the corona, which actually represents the percentage of the unmasked solar radiation at a given time (UT) and location (h, Φ, θ). To calculate the value of the F_R(UT, h, Φ, θ), we first calculate the eclipse magnitude at a given time and location by a JavaScript Eclipse Calculator, which is a java program developed by Chris O'Byrne and Stephen McCann with the open source code on the web site (http://www.chris.obyrne.com/Eclipses/calculator.html). When the eclipse magnitude at any moment and any location is known, according to the astronomical model of Curto et al. (2006), we can calculate the F_R(UT, h, Φ, θ) at the corresponding time and location. Figure 1 illustrates the distribution of the revised eclipse factor F_R(UT, h, Φ, θ) at an altitude of 200 km in the 1.67° E meridian as a function of UT and geographic latitude. As shown in Fig. 1, a total eclipse occurred at 48.9° N with a percentage of 22% of the solar radiation emitted by the unmasked part of the solar corona at the eclipse totality, and there was a partial eclipse between 20° N and 48.9° N. For a partial eclipse, a maximum eclipse is the instant when the greatest fraction of the Sun's diameter is occulted. For a total eclipse, maximum eclipse is the instant of mid-totality. From Fig. 1 one can find that around the time of UT=10.35 (10:21 UT), there occurs a maximum eclipse for all eclipse regions between 20° N and 60° N in the 1.67° E meridian.

The simulation was carried out in a magnetic plane (n_p, n_l) (n_p=201, n_l=100), where n_p is the number of points along a magnetic field line, n_l is the number of magnetic field lines, with a time step of 60 s. The geomagnetic longitude of the magnetic plane is 70° E, the associated geographic longitude 1.67° E. The geomagnetic latitude ranges from 55° S to 55° N. The following geophysical parameters on 11 August 1999 are adopted: F10.7=130.8, F10.7A=164.5, 3 h geomag-
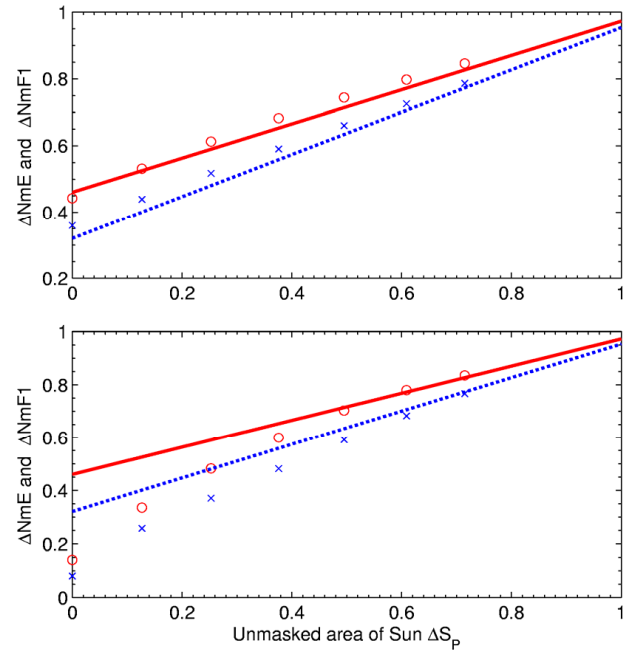

Fig. 3. Comparison of linear fit for the observed ΔNmE (solid line) and ΔNmF1 (dotted line) which is the same as Fig. 2 with the modelled ΔNmE (circles) and ΔNmF1 (crosses) by using the revised eclipse factor F_R (Top) and the unrevised eclipse factor F (Bottom), respectively.

netic index AP=(12, 7, 3, 4, 4, 4, 9, 6). We run a simulation with the revised eclipse factor F_R(UT, h, Φ, θ) described above, with the results denoted by subscript E (on eclipse day). In order to identify the effects of the eclipse, a further simulation was run for identical conditions but excluding the eclipse shadow, with the results denoted by subscript C (on control day). In addition, we run a simulation with the unrevised eclipse factor F(UT, h, Φ, θ) to compare the result with that of using F_R(UT, h, Φ, θ).

4 Results and discussions

4.1 Ionospheric response at the time of maximum eclipse

The data of foE and foF1(in Hz) from the ionosonde stations listed in Table 1 are transformed to the peak electron densities of the E layer and F1 layer, NmE and NmF1(in m^{-3}), by the equation f_o=9 Nm$^{1/2}$ (Rishbeth and Garriot, 1969), respectively. Figure 2 shows the dependence of the measured ΔNmE (NmE$_E$/NmE$_C$) and ΔNmF1 (NmF1$_E$/NmF1$_C$) on the ΔS$_P$ (SP$_E$/SP$_C$, the fraction of the Sun's area unmasked by the Moon). The solid line in Fig. 2 is a linear fit for ΔNmE and the dashed line for ΔNmF1. As illustrated in Fig. 2, the observed results show that the more the area of the Sun which is eclipsed (that is, the less ΔS$_P$), the greater the changes are in NmE and NmF1. It is seen that for the same ΔS$_P$,

ΔNmF1 is always smaller than ΔNmE from the figure. At totality (ΔS_P=0), ΔNmE falls to about 0.46 and ΔNmF1 falls to about 0.32. Furthermore, for each ionosonde station which records both NmE and NmF1, ΔNmF1 is also smaller than ΔNmE. In conclusion, during an eclipse the relative response of the electron density in the F1 layer is greater than that in the E layer.

In Fig. 3, we plot the linear fit for the observations (as shown in Fig. 2) and the modeled ΔNmE and ΔNmF1. The modeled results from using the revised eclipse factor F_R are plotted in the upper panel and the modelled results from using the unrevised eclipse factor F are plotted in the bottom panel. The seven modelled results plotted in Fig. 3 are for locations over 29.6° N, 32.7° N, 35.8° N, 39.0° N, 42.2° N, 45.5° N, and 48.9° N, respectively, with the maximum eclipse magnitude of 0.4, 0.5, 0.6, 0.7, 0.8, 0.9 and 1.0, respectively. From Fig. 3, one can find that the revised eclipse factor F_R makes the modelled results in accord with the measured results, whereas the unrevised eclipse factor F results in a large deviation between the modelled results and the measured ones. It can be concluded that, the revised eclipse factor F_R is fairly accurate for the description of the variation in solar radiations. As shown in Fig. 3, the modelled results suggest that there is a larger decrease in NmF1 than in NmE, which is in accord with the measured results. A similar result was reported by Roble et al. (1986). Both measured and modelled results reveal that during the eclipse the response of electron density in the F1 layer is larger than that in the E layer.

It is now well known that the E and F1 region are mainly dominated by the photochemical process, so ionospheric parameters NmE and NmF1 should be sensitive to changes in radiations caused by a solar eclipse. Both observations (as shown in Fig. 2) and calculations (as shown in Figs. 3 and 4) show that there are marked decreases in NmE and NmF1, though only a partial eclipse with a small eclipse magnitude occurred.

Given that the E-region behaves like an α-Chapman layer, the electron density in the E-region on the eclipse day and control day satisfies Eqs. (1) and (2), respectively:

$$\frac{d\mathrm{Ne}_E}{dt} = F_R \cdot q_0(\chi) - \alpha \cdot \mathrm{Ne}_E^2 \qquad (1)$$

$$\frac{d\mathrm{Ne}_C}{dt} = q_0(\chi) - \alpha \cdot \mathrm{Ne}_C^2 \qquad (2)$$

where Ne_E and Ne_C are the electron density on the eclipse day and control day, $q_0(\chi)$ is the normal production rate, χ is the solar zenith angle, F_R is the eclipse factor defined in Sect. 3, and α is the recombination rate coefficient. The solar eclipse is not a very rapid variation process; take the 11 August 1999 eclipse, for example, for a given place, such as 49.8° N and 1.67° E, it took more than three hours to cover the whole eclipse process from the eclipse begin to the eclipse end. So we can assume a quasi-stationary state for
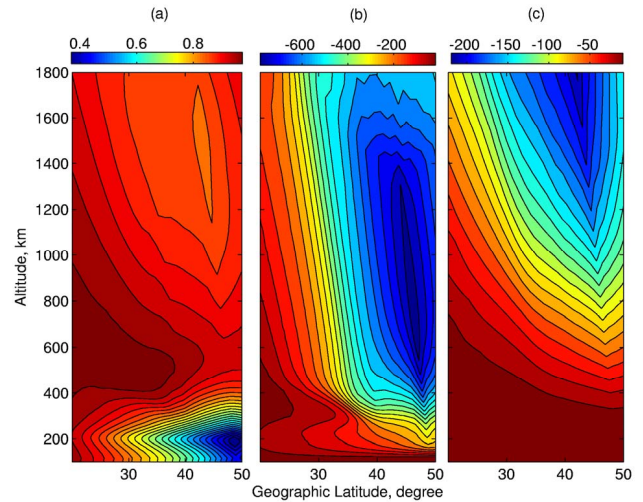

Fig. 4. Contours of the relative change in electron density **(a)**, $\mathrm{Ne}_E/\mathrm{Ne}_C$, electron temperature **(b)**, $\mathrm{Te}_E - \mathrm{Te}_C$, and ion O^+ drift velocity along field line (positive upward) **(c)**, $\mathrm{ViO}_E - \mathrm{ViO}_C$, as a function of geographic latitude and altitude at 10:21 UT. The longitude is about 1.67° E. These results are calculated by the ionospheric model.

the eclipse that the left sides of the continuity Eqs. (1) and (2) become zero. Under the assumption of a quasi-stationary state, from Eqs. (1) and (2) we can obtain the relative decrease in electron density ΔNmE$=\mathrm{Ne}_E/\mathrm{Ne}_C=F_R^{1/2}$. At totality, the F_R reaches a minimum of about 0.22, so the minimum ΔNmE$\approx$0.47. This value is consistent with both the result derived from the linear fit of the observations (about 0.46) and the modeling result (about 0.446).

The F1 region lies at a region of transition from the "square law" loss formula αN^2 to the "linear" formula βN (Ratcliffe, 1956; Rishbeth, 1968). If the F1-region is governed by a linear loss βN, the relative decrease in electron density $\mathrm{Ne}_E/\mathrm{Ne}_C$ is equal to F_R, i.e. at totality the ΔNmF1 is 0.22 under the assumption of a linear loss βN. And if the F1-region is governed by a square low loss αN^2, at totality the value of the ΔNmF1 would be 0.47. The square law loss αN^2 and the linear loss βN are equally important in the F1-region. Therefore, at totality the ΔNmF1 should be equal to a value between 0.22 and 0.47. The corresponding values of ΔNmF1 derived from observations and calculations are 0.32 and 0.37, respectively, which agrees with the discussion above.

The modelled relative changes in electron density (Ne), electron temperature (Te), and ion O^+ drift velocity along the field line (Vi) on the 1.67° E meridian at 10:21 UT are illustrated in Fig. 4. The change in Ne is defined as ΔNe=$\mathrm{Ne}_E/\mathrm{Ne}_C$, the change in Te is defined as ΔTe=$\mathrm{Te}_E-\mathrm{Te}_C$, and the change in Vi (positive upward) is defined as ΔVi=$\mathrm{Vi}_E-\mathrm{Vi}_C$. As shown in Fig. 4a, most of the relative decreases in electron density occur in altitudes lower than
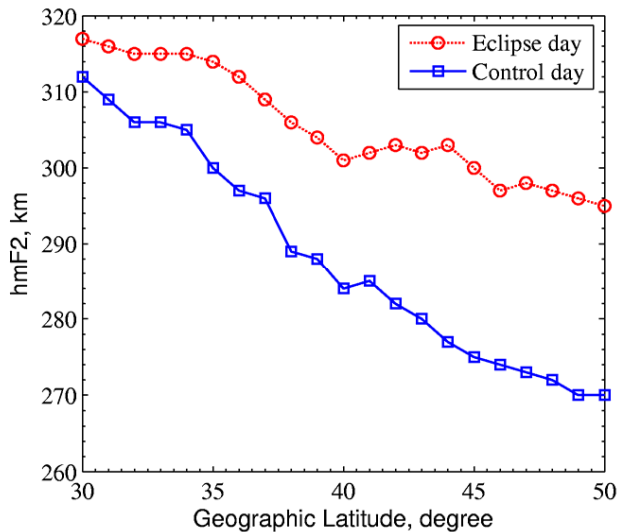
Fig. 5. The values of the hmF2 at 10:21 UT on eclipse day (dashed circle line) and on control day (solid square line) versus geographic latitude.

Fig. 6. The simulated ionospheric response to the solar eclipse at latitude of 48.8° N. Time evolution of the relative change in electron density **(a)**, NeE/NeC, electron temperature **(b)**, TeE–TeC, and ion O+ drift velocity along field line (positive upward) **(c)**, ViOE–ViOC. Circles on the x-axis indicate the time of the commencement, totality and end of solar eclipse, respectively.

400 km and the largest change with ΔNe=0.343 is attained at an altitude of about 185 km over 48.8° N; there is little response with ΔNe larger than 0.9 in the altitude range of 400 km–800 km; and there is also an obvious decrease in electron density with ΔNe≈0.85 at a higher altitude range of 1200 km–1800 km. From Fig. 4a, we can find that over all "eclipse" regions (from 20° N to 60° N) the largest change in electron density is in the range of 180–200 km (F1 region). In addition, the height of this largest change rises with decreasing latitude from around 185 km over 50° N to around 205 km over 25° N. Calculations also show that, compared to the normal behavior on the control day, there is an increase in the peak height of the F2 layer, hmF2 (as shown in Fig. 5) over all regions at maximum eclipse. The greater the eclipse magnitude is, the larger the change in hmF2. For example, hmF2 at 33° N (partial eclipse with the eclipse magnitude of 0.5) rises from about 305 km to 315 km and hmF2 at 50° N (total eclipse) rises from about 270 km to 295 km. The similar results have been reported by Evans (1965b), Stubbe (1970), Salah et al. (1986), and Boitman et al. (1999). As shown in Fig. 4a, for the height range between 200 km and 400 km, the lower the height is, the larger the magnitude of the decrease in electron density, i.e. the decrease in electron densities at altitudes below the hmF2 is greater than that at latitudes above the hmF2, which causes a change in the shape of the height profile of the electron density and a rise in hmF2.

Figure 4b shows an overall decrease in electron temperature throughout the entire height range except the E-region (below 140 km). The largest decrease in electron temperature occurs in the altitudes of 600–1000 km over about 46° N and reaches more than 700 K, whereas there is little drop
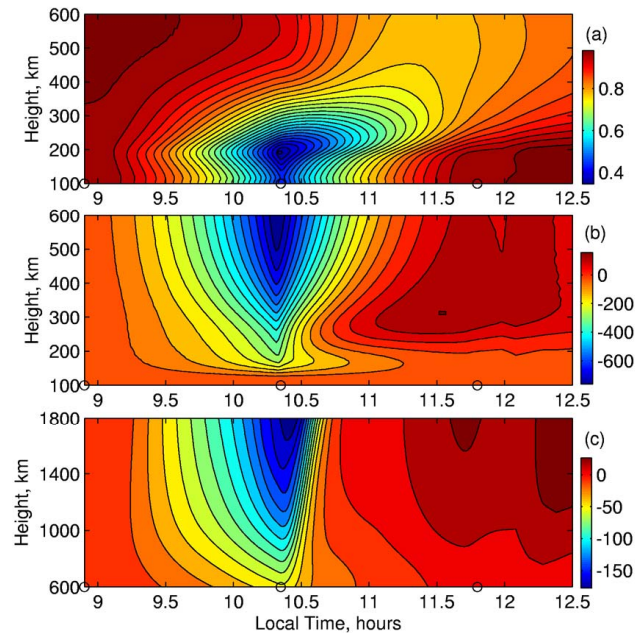
(less than 50 K) at low altitude (below 140 km). In addition, calculations show that ion temperature (not shown) also has a slight decrease of 100–200 K at heights above 600 km, whereas there is a slight decrease of less than 100 K at heights below 600 km. There are many similar reports about a large decrease in electron temperature and a smaller decrease in ion temperature derived from measurements and simulations as a consequence of the eclipse in the past (Evans, 1965a; Stubbe, 1970; Salah et al., 1986; Roble et al., 1986; Boitman et al., 1999). The calculated relative change in the ion drift velocity parallel to the magnetic field line is shown in Fig. 4c, where there is an overall downward ion flux at maximum eclipse (10:21 UT), with the largest downward ion drift velocity more than 200 m/s at an altitude of about 1800 km. In addition, the eclipse magnitude is smaller at the lower latitude, therefore the downward ion drift velocity is smaller there. It should be noted that this downward ion drift velocity is a relative value defined as Vi_E–Vi_C, where Vi_E is the ion drift velocity during the eclipse which is downward; Vi_C is the ion drift velocity on the control day which is upward. The large decrease in electron temperature and a smaller decrease in ion temperature would cause a corresponding fall in the value of the diffusive equilibrium scale height; therefore, it results in ionizations moving downward. The downward ionization flux makes up for electron losses at low heights and hence electron density decreases much less

in the topside ionosphere than at low heights (as shown in Fig. 4a). In addition, the downward ionization flux from the plasmasphere also leads to a decrease in electron density at this height (as shown in Fig. 4a).

4.2 Time-dependent response of the ionosphere to solar eclipse

As shown in Fig. 1, for $1.67°$ E meridian, during the solar eclipse of 11 August 1999 the strongest eclipse occurred at about $49°$ N. We plot time evolution of simulated ionospheric response to the solar eclipse in Fig. 6. Figure 6a shows the relative change in electron density ΔNe, Fig. 6b shows the relative change in electron temperature ΔTe, and Fig. 6c shows the relative change in ion O^+ drift velocity ΔVi (positive upward) along the field line. From Fig. 6a, one can find that during the whole eclipse, eclipse effects on the electron density mainly occur at altitudes below 600 km. The time when a minimum of ΔNe is attained is height dependent. For altitudes below 200 km (the E- and F1-region) it is approximately synchronous with the totality (about 10:21 UT), and at altitudes above 200 km it is markedly delayed with regard to the time of totality: the time lag between totality and the greatest reduction in Ne (corresponding minimum ΔNe) increases with the altitude and reaches a maximum at about 600 km and then becomes smaller again. For example, the time lag is 15 min at 300 km, 60 min at 600 km, and 30 min at 1200 km, which is coincident with the results from Stubbe (1970). It is now well known that such a delay feature of the ionosphere is related to the "sluggishness" of the ionosphere (Appleton, 1953; Rishbeth, 1968; Rishbeth and Garriott; 1969). It means that changes in Ne should theoretically lag behind changes in the electron production rate by a time constant of $1/2\alpha N$ for the low altitudes and $1/\beta$ for the high altitudes, where α is the square law loss coefficient and β is the linear loss coefficient. Figure 6a also shows that before the totality the height of the ΔNe minimum is at a constant altitude of about 200 km, whereas after that time it rises gradually with time. After totality the electron density at low heights begins to recover rapidly, whereas at high heights it still continues to decrease due to the time lag mentioned above, so the height of the ΔNe minimum rises with time. Calculations also show that hmF2 rises with time, reaches a peak, and then decreases gradually to the usual daytime level at the end of the eclipse. The largest rise in hmF2 is about 25 km at 10:24 UT, i.e. the time delay of hmF2 response does not exceed 3 min.

Figure 6b presents the calculated height-time variation in ΔTe during the eclipse. Calculations show that the beginning of the eclipse occurs simultaneously with an overall decrease in electron temperature throughout the entire height range. At all heights changes in electron temperature are synchronous with the eclipse magnitude. The largest drop in electron temperature occurs at the time of totality. The typical value of ΔTe is about -200 K at 200 km, -500 K at
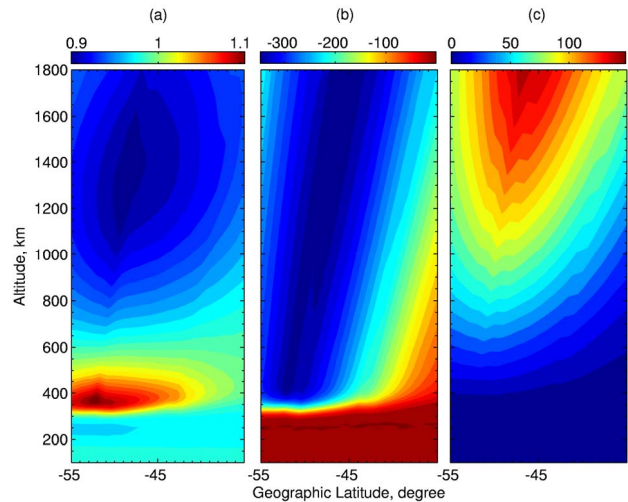

Fig. 7. Same as Fig. 4, but for the conjugate hemisphere ($35°$ S–$55°$ S).

400 km, and -700 K at 600 km. After the totality the electron temperature begins to increase gradually and recovers to the usual daytime level before the end of the eclipse. Furthermore, calculations show that the electron temperature continues to increase with the largest positive ΔTe of about 100 K, as shown in Fig. 6b, at the end of the eclipse. At this time, solar irradiation recovers to the usual level entirely; however, electron density is still relatively low, owing to recombination, which causes a small increase in Te. These results are similar to the increase in Te at sunrise.

The height-time variation in the calculated ion drift velocity difference ΔVi is shown in Fig. 6c. Due to a decrease in the diffusive equilibrium scale height which is caused by a decrease in electron and ion temperature, the ion in the higher altitudes moves downwards to make up for ion losses in the lower ionosphere. As shown in Fig. 6c, the largest ion flux downwards occurs at totality for all height ranges. With the recovery of electron density and temperature, the ion flux downwards decreases gradually. The lower ionosphere recovers much faster than the upper ionosphere, which causes the downward velocity to diminish. Near the end of the eclipse, the ion drift velocity may even change its direction at higher altitudes due to the recovery of the electron density and the small increase in electron temperature.

4.3 Ionospheric disturbances in the conjugate hemisphere

Simulated results show that there are also ionospheric disturbances in the conjugate hemisphere when the eclipse occurs in the Northern Hemisphere. Figure 7 shows the relative change in electron density ΔNe, electron temperature ΔTe, and ion O^+ drift velocity ΔVi in the regions of $35°$ S–$55°$ S at 10:21 UT. Figure 7a shows that a small decrease in electron density occurs in the plasmasphere with the greatest decrease

value of $\Delta Ne \approx 0.9$ at altitudes of 1200–1400 km, at the same time a small increase in electron density occurs in the F region with the greatest increase value of $\Delta Ne \approx 1.1$ at about 380 km. In the Northern Hemisphere the total eclipse occurs at about 49° N, and its magnetic conjugate point is at 53° S. So the associated greatest disturbance in the Southern Hemisphere should occur at 53° S (as shown in Fig. 7a). Calculations show that the greatest disturbance in electron density is delayed about 12 min compared to the time of maximum eclipse (10:21 UT). Figure 7b shows the there is an overall decrease in electron temperature at altitudes above 300 km in the conjugate hemisphere. The greatest decrease corresponding to the value of $\Delta Te \approx 350$ K occurs in the region along geomagnetic field lines with the footpoints near 53° S. Simulations show that the greatest disturbance in electron temperature is almost synchronous, with the eclipse occurring in the Northern Hemisphere. As illustrated in Fig. 7c, there is an overall ion flux downward along the geomagnetic field line at altitudes above 400 km in the conjugate hemisphere.

Energetic photoelectrons are created during the photoionization of the neutral gases and heat the ambient electron gas. At lower altitudes, most of the photoelectron heat is distributed locally. At higher altitudes, the more energetic photoelectrons are able to propagate along the magnetic field lines, heating the gas further afield with observable effects in the conjugate hemisphere (Millward et al., 1993). The phenomenon of the energetic photoelectron flow from a conjugate sunlit hemisphere to a darkness hemisphere has been mentioned and considered in some papers in the past (e.g. Evans, 1973; Schunk and Nagy, 1978; Bailey and Sellek, 1990; Chao et al., 2003, Zhang et al., 2004; Lei et al., 2007; Bilitza et al., 2007). When the Northern Hemisphere is in darkness during the eclipse, the magnetic conjugate-points in the Southern Hemisphere are still illuminated. The sunlit asymmetry between the two hemispheres causes an asymmetry of the distribution of photoelectron in the two hemispheres. Due to the decrease in solar radiations, the photoelectron production rate in the Northern Hemisphere decreases by a large magnitude at eclipse totality, which therefore causes a corresponding decrease in the photoelectron travelling along the magnetic field lines to the Southern Hemisphere and the heating of electron gas there. So at higher altitudes in the Southern Hemisphere, the electron heating rate would decrease due to the large decrease in the photoelectron heating from the Northern Hemisphere, which causes a decrease in electron temperature, as shown in Fig. 7b. At lower altitudes in the Southern Hemisphere, the electron temperature is not affected during the eclipse process at the Northern Hemisphere, since the local heating effect occurs at lower altitudes. For the Southern Hemisphere, the decrease in electron temperature causes a corresponding decrease in the scale height of plasma, which makes a redistribution of plasma and leads to a plasma flow downward along the geomagnetic field line (as shown in Fig. 7c), and therefore a small decrease in electron density in the

plasmasphere and a small increase in electron density in the F region (as shown in Fig. 7a).

Given the variable nature of the F region, a small increase in electron densities by only ∼10% is hard to observe and therefore to validate. As for the 11 August 1999 solar eclipse event, its path of totality passing over central Europe, the conjugate hemisphere therefore locates over the southern Atlantic Ocean where there are no ionospheric observatories at all. As is known, there are far more ionospheric observatories in the Northern Hemisphere than in the southern hemisphere. For a solar eclipse event in the Southern Hemisphere, it might be possible to obtain more ionospheric data in the conjugate hemisphere and test this prediction. Given enough ionospheric stations worldwide, it might be possible to make the results statistically significant and we will continue to do relevant work later.

5 Summary

Using the data from 16 ionosonde stations in Europe, we perform a statistical analysis of the response of the E- and F1-region to the 11 August 1999 eclipse. Then according to the astronomical model of Curto et al. (2006), we construct a revised eclipse factor F_R(UT, h, Φ, θ), which is equal to the ratio of the unmasked solar radiation to the total solar radiation, taking account of the radiation from the solar corona when calculating the total solar radiation. A middle and low latitude theoretical ionospheric model and the eclipse factor F_R are used to model the ionospheric response to this eclipse. Both the observations and the calculations show that for the mid- and low latitude ionosphere, the decrease in the electron density during a solar eclipse is greater in the F1-region than in the E-region. The simulations show that except the obvious ionospheric response at low altitudes below 500 km, there is also a small response at high altitudes up to about 2000 km. In addition, calculations show that when the eclipse takes place in the Northern Hemisphere there is also a small ionospheric disturbance in the conjugate hemisphere. The main simulated results are summarized as follows:

1. For the mid- and low latitude ionosphere, the decrease in the electron density during solar eclipse is greater in the F1 region than in the E region. The electron density at the altitude range of 1500–1800 km also decreases slightly. The eclipse also causes a marked drop in electron temperature at altitudes above 200 km, with the largest drop of about 700 K in the topside ionosphere, while the ion temperature decreases slightly.

2. The decreases in electron densities in the E- and F1-region are nearly synchronous with the eclipse function, whereas the F2-region responds to the eclipse with an obvious time lag, which is about 15 min at 300 km, 60 min at 600 km, and 30 min at 1200 km. The change in electron temperature over the entire height range is

synchronous with the eclipse function, and it begins to increase at 30 min after the totality and reaches the largest value of about 200 K at the end of eclipse.

3. For the conjugated hemisphere, the electron density decreases slightly in the latitudes of 300–500 km and increases slightly in the latitudes of 1200–1600 km, and there is also an overall decrease in electron temperature with the largest value of about 300 K.

References

Adeniyi, J. O., Radicella, S. M., Adimula, I. A., Willoughby, A. A., Oladipo, O. A., and Olawepo, O.: Signature of the 29 March 2006 eclipse on the ionosphere over an equatorial station, J. Geophys. Res., 112, A06314, doi:10.1029/2006JA012197, 2007.

Afraimovich, E. L., Palamartchouk, K. S., Perevalova, N. P., Chemukhov, V. V., Lukhnev, A. V., and Zalutsky, V. T.: Ionospheric effects of the solar eclipse of March 9, 1997, as deduced from GPS data, Geophys. Res. Lett., 25(4), 465–468, 1998.

Afraimovich, E. L., Kosogorov, E. A., and Lesyuta, O. S.: Effects of the August 11, 1999 total solar eclipse as deduced from total electron content measurements at the GPS network, J. Atmos. Sol.-Terr. Phy., 64, 1933–1941, 2002.

Appleton, E. V.: A note on the "sluggishness" of ionosphere, J. Atmos. Terr. Phys., 3, 228–232, 1953.

Bailey, G. J. and Sellek, R. A.: Mathematical model of the Earth's plasmasphere and its application in a study of He+ at L = 3.0, Ann. Geophys., 8, 171–190, 1990,
http://www.ann-geophys.net/8/171/1990/.

Baran, L. W., Ephishov, I. I., Shagimuratov, I. I., Ivanov, V. P., and Lagovsky, A. F.: The response of the ionospheric total electron content to the solar eclipse on August 11, 1999, Adv. Space Res., 31(4), 989–994, 2003.

Bilitza, D., Truhlik, V., Richards, P., Abe, T., and Triskova, L.: Solar cycle variations of mid-latitude electron density and temperature: Satellite measurements and model calculations, Adv. Space Res., 39, 779–789, 2007.

Boitman, O. N., Kalikhman, A. D., and Tashchilin, A. V.: The midlatitude ionosphere during the total solar eclipse of March 9, 1997, J. Geophys. Res., 104(A12), 28 197–28 206, 1999.

Chao, C. K., Su, S.-Y., and Yeh, H. C.: Presunrise ion temperature enhancement observed at 600 km low and mid-latitude ionosphere, Geophys. Res. Lett., 30(4), 1187, doi:10.1029/2002GL016268, 2003.

Cheng, K., Huang, Y.-N., and Chen, S.-W.: Ionospheric effects of the solar eclipse of September 23, 1987, around the equatorial anomaly crest region, J. Geophys. Res., 97(A1), 103–111, 1992.

Cohen, E. A.: The study of the effect of solar eclipses on the ionosphere based on satellite beacon observations, Radio Sci., 19, 3, 769–777, 1984.

Curto, J. J., Heilig, B., and Pinol, M.: Modeling the geomagnetic effects caused by the solar eclipse of 11 August 1999, J. Geophys. Res., 111, A07312, doi:10.1029/2005JA011499, 2006.

Davis, C. J., Lockwood, M., Bell, S. A., Smith, J. A., and Clarke, E. M.: Ionospheric measurements of relative coronal brightness during the total solar eclipses of 11 August, 1999 and 9 July, 1945, Ann. Geophys., 18, 182–190, 2000,
http://www.ann-geophys.net/18/182/2000/.

Davis, C. J., Clarke, E. M., Bamford, R. A., Lockwood, M., and Bell, S. A.: Long term changes in EUV and X-ray emissions from the solar corona and chromosphere as measured by the response of the Earth's ionosphere during total solar eclipses from 1932 to 1999, Ann. Geophys., 19, 263–273, 2001,
http://www.ann-geophys.net/19/263/2001/.

Evans, J. V.: An F Region Eclipse, J. Geophys. Res., 70, 131–142, 1965a.

Evans, J. V.: On the Behavior of foF2 during Solar Eclipses, J. Geophys. Res., 70, 733–738, 1965b.

Evans, J. V.: Seasonal and sunspot cycle variation of F region electron temperatures and protonospheric heat flux, J. Geophys. Res., 78, 2344–2349, 1973.

Farges, T., Jodogne, J. C., Bamford, R., Roux Y. Le., Gauthier, F., Vila, P. M., Altadill, D., Sole, J. G., and Miro, G.: Disturbances of the western European ionosphere during the total solar eclipse of 11 August 1999 measured by a wide ionosonde and radar network, J. Atmos. Sol.-Terr. Phy., 63, 915–924, 2001.

Farges, T., Pichon, A. Le, Blanc, E., Perez, S., and Alcoverro, B.: Response of the lower atmosphere and the ionosphere to the eclipse of August 11, 1999, J. Atmos. Sol.-Terr. Phy., 65, 717–726, 2003.

Hedin, A. E., Fleming, E. L., Manson, A. H., et al.: Empirical wind model for the upper, middle and lower atmosphere, J. Atmos. Terr. Phys., 58, 1421–1447, 1996.

Huang, C. R., Liu, C. H., Yeh, K. C., Lin, K. H., Tsai, W. H., Yeh, H. C., and Liu, J. Y.: A study of tomographically reconstructed ionospheric images during a solar eclipse, J. Geophys. Res., 104(A1), 79–94, 1999.

Hunter A. N., Holman, B. K., fieldgate, D. G., and Kelleher, R.: Faraday rotation studies in Africa during the solar eclipse of June 30, 1973, Nature, 250, 205–206, 1974.

Klobuchar, J. A. and Whitney, H. E.: Ionospheric electron content measurements during a solar Eclipse, J. Geophys. Res., 70(5), 1254–1257, 1965.

Korenkov, Y. N., Klimenko, V. V., Baran, V., Shagimuratov, I. I., and Bessarab, F. S.: model calculations of TEC over Europe during 11 August 1999 solar eclipse, Adv. Space Res., 31(4), 983–988, 2003a.

Korenkov, Y. N., Klimenko, V. V., Bessarab, F. S., Nutsvalyan, N. S., and Stanislawska, I.: Model/data comparison of the F2-region parameters for the 11 August 1999 solar eclipse, Adv. Space Res., 31(4), 995–1000, 2003b.

Lei, J., Liu, L., Wan, W., and Zhang, S. R.: Modeling the behavior of ionosphere above Millstone Hill during the September 21-27, 1998 storm, J. Atmos. Sol.-Terr. Phy., 66, 1093–1102, 2004a.

Lei, J., Liu, L., Wan, W., and Zhang, S. R.: Model results for the ionospheric lower transition height over mid-latitude, Ann. Geo-

phys., 22, 2037–2045, 2004b.

Lei, J.: Statistical analysis and modeling investigation of middle latitude ionosphere. Dissertation for the Doctoral Degree. Beijing: Institute of Geology and Geophysics, Chinese Academy of Sciences, 2005.

Lei, J., Roble, R. G., Wang, W., Emery, B. A., and Zhang, S.-R.: Electron temperature climatology at Millstone Hill and Arecibo, J. Geophys. Res., 112, A02302, doi:10.1029/2006JA012041, 2007.

Liu, L., Wan, W., Tu, J. N., Bao, Z. T., and Yeh, C. K.: Modeling study of the ionospheric effects during a total solar eclipse, Chinese J. Geophys, 42(3), 296–302, 1999.

Millward, G. H.: A global model of the earth's thermosphere, ionosphere and plasmasphere: theoretical studies of the response to enhanced high-latitude convection, Dissertation for the Doctoral Degree, UK: University of Sheffield, 1–195, 1993.

Müller-Wodarg, I. C. F., Aylward, A. D., and Lockwood, M.: Effects of a Mid-Latitude Solar Eclipse on the Thermosphere and Ionosphere – A Modelling Study, Geophys. Res. Lett., 25(20), 3787–3790, 1998.

Oliver, W. L. and Bowhill, S. A.: The F1 region during a solar eclipse, Radio. Sci., 9(2), 185–195, 1974.

Picone, J. M., Hedin, A. E., Drob, D. P., and Aikin, A. C.: NRLMSISE-00 empirical model of the atmosphere: statistical comparisons and scienti5c issues, J. Geophys. Res., 107(A12), 1468, doi:10.1029/2002JA009430, 2002.

Ratcliffe, J. A.: The formation of the ionospheric layers F1 and F2, J. Atmos. Terr. Phys., 8, 260–269, 1956.

Richards, P. G., Fennelly, J. A., and Torr, D. G.: EUVAC: A Solar EUV Flux Model for Aeronomic Calculations, J. Geophys. Res., 99, 8981–8992, 1994.

Rishbeth, H.: Solar eclipses and ionospheric theory, Space. Sci. Rev., 8(4), 543–554, 1968.

Rishbeth, H. and Garriott, O. K.: Introduction to Ionospheric Physics, Academic Press, San Diego, CA, 1969.

Roble, R. G., Emery, B. A., and Ridley, E. C.: Ionospheric and Thermispheric Response Over Millstone Hill to the May 30, 1984, Annular Solar Eclipse, J. Geophys. Res., 91(A2), 1661–1670, 1986.

Salah, J. E., Oliver, W. L., Foster, J. C., and Holt, J. M.: Observations of the May 30, 1984, Annular Solar Eclipse at Millstone Hill, J. Geophys. Res., 91(A2), 1651–1660, 1986.

Schunk, R. W. and Nagy, A. F.: Electron temperatures in the F region ionosphere: Theory and observations, Rev. Geophys., 16, 355–399, 1978.

Stubbe, P.: The F-region during an eclipse – A theoretical study, J. Geophys. Res., 32, 1109–1116, 1970.

Titheridge, J. E.: Model results for the ionospheric E-region: solar and seasonal changes, Ann. Geophys., 15, 63–78, 1997, http://www.ann-geophys.net/15/63/1997/.

Tomás, A. T., Lühr, H., Förster, M., Rentz, S., and Rother, M.: Observations of the low-latitude solar eclipse on 8 April 2005 by CHAMP, J. Geophys. Res., 112, A06303, doi:10.1029/2006JA012168, 2007.

Tsai, H. F. and Liu, J. Y.: Ionospheric total electron content response to solar eclipses, J. Geophys. Res., 104(A6), 12 657–12 668, 1999.

Tu, J. N., Liu, L., and Bao, Z. T.: An low latitude theoretical ionospheric model, Chinese J. Space Sci (in Chinese), 17, 212–219, 1997.

Yue, X., Wan, W., Liu, L., Le, H., Chen, Y., and Yu, T.: Development of a middle and low latitude theoretical ionospheric model and an observation system data assimilation experiment, Chinese Sci. Bull., 53(1), 94–101, 2008.

Zhang, S.-R., Holt, J. M., Zalucha, A. M., and Amory-Mazaudier, C.: Midlatitude ionospheric plasma temperature climatology and empirical model based on Saint Santin incoherent scatter radar data from 1966 to 1987, J. Geophys. Res., 109, A11311, doi:10.1029/2004JA010709, 2004.